

# Effects of Synchronization Error on Space Time Block Codes Equipped with FSK Waveforms

Chris Potter  
Dynerics, Inc.  
Huntsville, AL

Kurt Kosbar  
Missouri S&T, Rolla, MO

Adam Panagos  
Dynerics, Inc.  
Huntsville, AL

## ABSTRACT

Space-time Coding (STC) for Multiple-Input Multiple-Output (MIMO) wireless communication systems is an effective technique for providing robust wireless link performance in telemetry systems. This paper investigates the degradation in system performance when synchronization errors between the transmitter and receiver are present. Specifically, expressions that quantify the increase in symbol-error-rate as a function of symbol synchronization error are derived for a two-transmit and single receive antenna MISO system using binary frequency shift keying waveforms. These results are then extended to the MIMO case. The analytic results are verified with simulation results that show close agreement between the theoretical expressions and Monte Carlo simulation runs.

## KEY WORDS

space-time coding, multiple-input multiple-output, frequency shift keying, synchronization, probability of error

## INTRODUCTION

Many telemetry systems must establish reliable communications through challenging radio frequency channels. Noise, multipath, fading, nonlinear distortion and interference are all commonly encountered. One way to mitigate many of these problems, is to use multiple antennas at the transmitter and receiver locations [1, 2]. These multiple-input multiple-output (MIMO) systems can overcome deep fades, and allow the designer to tradeoff increased data reliability with higher throughput [3, 4].

As helpful as MIMO techniques can be, they come at a cost. The amount of radio frequency hardware at the transmitter and receivers is typically proportional to the number of antennas at each location. The complexity of the baseband signal processor at the receiver can also be substantially higher than in conventional single-input, single-output (SISO) systems. If the receiver and transmitter can not develop accurate estimates of the channel characteristics, then it can be difficult to see the promised gains [5]. The particular challenge investigated in this paper is how the MIMO gains may be reduced due to symbol synchronization errors at the receiver.

All digital communication systems require the receiver to form an estimate of when each transmitted symbol begins, and ends. Many of the calculations of channel capacity, and error rate performance, are only valid when the synchronization errors are negligible. A variety of synchronization architectures have been developed for digital communication systems. Regardless of which synchronization technique is used, it is inevitable that some symbol synchronization error will remain. This will degrade MIMO performance in two ways. It will essentially introduce inter-symbol interference, as the receiver is influenced by the bits adjacent to the one being demodulated. In addition, errors will be made in the channel estimation algorithm, which will indirectly influence the error rate.

This paper presents an analytical framework, and numerical simulation results, for analyzing and measuring the degradation of symbol error rate as a function of synchronization errors for MIMO systems utilizing frequency shift keying (FSK) with space time block codes (STBC). This work extends the work of [6] in two key aspects. The first is generalizing the channel estimation and decoding techniques from a multiple-input single-output (MISO) system to a MIMO architecture. The second is the analysis (through both mathematics and computer simulation) of system performance when synchronization errors are present. These new results are the main focus of this work.

## INPUT-OUTPUT DESCRIPTION

A MIMO wireless baseband flat fading communication system with  $N_r$  receive antennas and  $N_t$  transmit antennas is modeled at time  $t$  by

$$\mathbf{r}(t) = \mathbf{H}(t)\mathbf{x}(t) + \mathbf{n}(t)$$

where  $\mathbf{r}(t)$  is the  $N_r \times 1$  received vector,  $\mathbf{x}(t)$  is the  $N_t \times 1$  transmitted symbol vector. The elements of the transmit vector can be written as  $s_i(t)$ , where each of these waveforms is a Frequency Shift Keyed (FSK) signal with symbol energy  $E_s$ . The channel noise is written as  $\mathbf{n}$ , which is a vector of size  $N_r \times 1$  each term being a independent, identically distributed complex gaussian number,  $n_i \stackrel{iid}{\sim} \mathcal{CN}(0, N_o)$ . The gain, and phase shift, between each of the  $n^{th}$  transmit antennas and the  $m^{th}$  receive antennas is captured in the  $N_r \times N_t$  channel matrix  $\mathbf{H}(t) = \{h_{mn}(t)\}$ .

In this work, we assume the transmitted bandwidth is narrow enough that the channel induces flat frequency fading, with a temporal correlation modeled by Jakes [7]. Specifically, each sub-channel autocorrelation function satisfies

$$R_{g_{mn}g_{mn}}(\tau) = J_0(2\pi f_d T_s \tau),$$

where  $f_d$  is the doppler frequency and  $T_s$  is the symbol period. To keep the analysis and simulations tractable, for the remainder of this work we will use a MIMO system with two transmit and two receive antennas - in other words  $N_t = N_r = 2$ .

## SYNCHRONIZATION ERROR

In this work, there are two different types of synchronization errors that will be encountered. The first is an error in the symbol period. This is modeled by

$$\hat{T} \triangleq T + \epsilon(t)$$

where  $\epsilon(t)$  is the symbol synchronization error. We will examine only the case where this type of error is a constant. The second type of error is timing offset of the symbol period. This is when the receiver has a very accurate estimate of the symbol period but is uncertain of where this period starts. In this case the error term will be written as  $T_o(t)$ , and we will examine the cases where this term is a constant, and also when it has a gaussian distribution.

## FSK WAVEFORMS

The baseband FSK signals for the  $i^{th}$  waveform is [8]

$$s_i(t) = \sqrt{\frac{2E_s}{T}} \exp(j2\pi(2i - M - 1)\Delta ft), \quad (k - 1)T \leq t \leq kT \quad (1)$$

where  $\Delta f$  is frequency separation between signals and the following transformation for index  $i$  has been made

$$i \mapsto 2i - M - 1.$$

To establish orthogonality between signals, it is routine to show that the minimum frequency separation is  $\Delta f = \frac{1}{2T}$ . For the purposes of this work, only binary FSK ( $M = 2$ ) will be considered. This simplifies (2) to

$$s_i(t) = \sqrt{\frac{2E_s}{T}} \exp\left(\frac{j\pi t(-1)^i}{T}\right), \quad (k - 1)T \leq t \leq kT.$$

which will prove useful for channel estimation and decoding.

## STBC

An Alamouti-type STBC [9] using FSK waveforms was described for a 1x2 MIMO system by [6]

$$\mathbf{X}(t) = \begin{bmatrix} x_1(t) & -x_2^*(t) \\ x_2(t) & x_1^*(t) \end{bmatrix}$$

where  $x_i(t)$ ,  $i = 1, 2$  belong to  $\mathcal{C}$ . Although the same STBC can be implemented for a MIMO system with multiple receive antennas, additional signal processing is required for channel estimation and decoding due to the presence of additional channel coefficients. A contribution of this work is fulfilling this task to multiple receive antennas. This process will begin with channel estimation.

## - Channel Estimation

The acquisition of accurate channel estimates is crucial for good system performance. For the reason, the process is shown first when there are no synchronization errors. This is then followed respectively by symbol period errors and timing offsets.

### I) Perfect Synchronization

The received signal for  $2kT \leq t \leq (2k+1)T$  is

$$\mathbf{y}(t) = \begin{bmatrix} h_{11}(k)x_1(t) + h_{12}(k)x_2(t) \\ h_{21}(k)x_1(t) + h_{22}(k)x_2(t) \end{bmatrix} + \begin{bmatrix} n_1(t) \\ n_2(t) \end{bmatrix}$$

Then

$$\begin{aligned} z_1(t) &\triangleq \sqrt{\frac{2}{E_s T}} \int_{2kT}^{(2k+1)T} \mathbf{y}(t) \cos\left(\frac{\pi t}{T}\right) dt \\ &= \begin{bmatrix} h_{11}(k) \int_{2kT}^{(2k+1)T} x_1(t) \cos\left(\frac{\pi t}{T}\right) dt + h_{12}(k) \int_{2kT}^{(2k+1)T} x_2(t) \cos\left(\frac{\pi t}{T}\right) dt \\ h_{21}(k) \int_{2kT}^{(2k+1)T} x_1(t) \cos\left(\frac{\pi t}{T}\right) dt + h_{22}(k) \int_{2kT}^{(2k+1)T} x_2(t) \cos\left(\frac{\pi t}{T}\right) dt \end{bmatrix} \\ &+ \sqrt{\frac{2}{E_s T}} \begin{bmatrix} \int_{2kT}^{(2k+1)T} n_1(t) \cos\left(\frac{\pi t}{T}\right) dt \\ \int_{2kT}^{(2k+1)T} n_2(t) \cos\left(\frac{\pi t}{T}\right) dt \end{bmatrix} \\ &= \begin{bmatrix} h_{11}(k) + h_{12}(k) \\ h_{21}(k) + h_{22}(k) \end{bmatrix} + \sqrt{\frac{2}{E_s T}} \begin{bmatrix} \int_{2kT}^{(2k+1)T} n_1(t) \cos\left(\frac{\pi t}{T}\right) dt \\ \int_{2kT}^{(2k+1)T} n_2(t) \cos\left(\frac{\pi t}{T}\right) dt \end{bmatrix} \end{aligned}$$

Following the same procedure it follows for  $(2k+1)T \leq t \leq (2k+2)T$  that

$$z_2(t) = \begin{bmatrix} -h_{11}(k) + h_{12}(k) \\ -h_{21}(k) + h_{22}(k) \end{bmatrix} + \sqrt{\frac{2}{E_s T}} \begin{bmatrix} \int_{2kT}^{(2k+1)T} n_1(t) \cos\left(\frac{\pi t}{T}\right) dt \\ \int_{2kT}^{(2k+1)T} n_2(t) \cos\left(\frac{\pi t}{T}\right) dt \end{bmatrix}$$

Thus the channel estimates are

$$\hat{\mathbf{h}}_1(k) = 1/2(z_1(t) - z_2(t))$$

and

$$\hat{\mathbf{h}}_2(k) = 1/2(z_1(t) + z_2(t))$$

### II) Symbol Period Synchronization Error

When there is symbol synchronization error at the receiver, the FSK waveforms will have different symbol periods and hence will lose their orthogonality properties. The impact on performance is analyzed by first noting that there are two cases to consider

i)  $\epsilon < 0$ . For  $2kT \leq t \leq (2k+1)T$

$$z_1(t) = \sqrt{\frac{2}{E_s \hat{T}}} \int_{2k\hat{T}}^{(2k+1)\hat{T}} \mathbf{y}(t) \cos\left(\frac{\pi t}{\hat{T}}\right) dt.$$

It follows after several manipulations that

$$\int_{2k\hat{T}}^{(2k+1)\hat{T}} s_i(t) \cos\left(\frac{\pi t}{\hat{T}}\right) dt = \sqrt{\frac{E_s}{2\hat{T}}} \alpha_i$$

where

$$\alpha_i = (T + \epsilon(T)) \exp((-1)^i j \pi \epsilon(T)) \left( \operatorname{sinc} \left( \frac{\epsilon(T)}{2T} \right) - \operatorname{sinc} \left( \frac{1 + \epsilon(T)}{2T} \right) \right).$$

If  $\{a_k\}$  is a sequence whose components are equally likely drawn from  $\{-1, 1\}$ , then for  $2kT \leq t \leq (2k+1)T$

$$\begin{aligned} z_1(t) &= \frac{1}{\sqrt{T\hat{T}}} \begin{bmatrix} -h_{11}(k)\alpha_{a_{4k}} + h_{12}(k)\alpha_{a_{4k+1}} \\ -h_{21}(k)\alpha_{a_{4k}} + h_{22}(k)\alpha_{a_{4k+1}} \end{bmatrix} \\ &\quad + \sqrt{\frac{2}{E_s\hat{T}}} \begin{bmatrix} \int_{2k\hat{T}}^{(2k+1)\hat{T}} n_1(t) \cos\left(\frac{\pi t}{\hat{T}}\right) dt \\ \int_{2k\hat{T}}^{(2k+1)\hat{T}} n_2(t) \cos\left(\frac{\pi t}{\hat{T}}\right) dt \end{bmatrix} \end{aligned}$$

Likewise, for  $(2k+1)T \leq t \leq (2k+2)T$

$$\begin{aligned} z_2(t) &= \frac{1}{\sqrt{T\hat{T}}} \begin{bmatrix} -h_{11}(k)\alpha_{a_{4k+2}} + h_{12}(k)\alpha_{a_{4k+3}} \\ -h_{21}(k)\alpha_{a_{4k+2}} + h_{22}(k)\alpha_{a_{4k+3}} \end{bmatrix} \\ &\quad + \sqrt{\frac{2}{E_s\hat{T}}} \begin{bmatrix} \int_{(2k+1)\hat{T}}^{(2k+2)\hat{T}} n_1(t) \cos\left(\frac{\pi t}{\hat{T}}\right) dt \\ \int_{(2k+1)\hat{T}}^{(2k+2)\hat{T}} n_2(t) \cos\left(\frac{\pi t}{\hat{T}}\right) dt \end{bmatrix} \end{aligned}$$

ii)  $\epsilon > 0$ . For  $2kT \leq t \leq (2k+1)T$

$$z_1(t) = \sqrt{\frac{2}{E_s\hat{T}}} \int_{2k\hat{T}}^{(2k+1)\hat{T}} \mathbf{y}(t) \cos\left(\frac{\pi t}{\hat{T}}\right) dt + \sqrt{\frac{2}{E_s\hat{T}}} \int_{(2k+1)T}^{(2k+1)T+\hat{T}} \mathbf{y}(t) \cos\left(\frac{\pi t}{\hat{T}}\right) dt.$$

It follows after some effort that

$$\begin{aligned} z_1(t) &= \frac{1}{\sqrt{T\hat{T}}} \begin{bmatrix} h_{11}(k)(1 - \alpha_{a_{4k}}) + h_{12}(k)(1 + \alpha_{a_{4k+1}}) \\ h_{21}(k)(1 - \alpha_{a_{4k}}) + h_{22}(k)(1 + \alpha_{a_{4k+1}}) \end{bmatrix} \\ &\quad + \sqrt{\frac{2}{E_s\hat{T}}} \begin{bmatrix} \int_{2k\hat{T}}^{(2k+1)\hat{T}} n_1(t) \cos\left(\frac{\pi t}{\hat{T}}\right) dt \\ \int_{2k\hat{T}}^{(2k+1)\hat{T}} n_2(t) \cos\left(\frac{\pi t}{\hat{T}}\right) dt \end{bmatrix} \end{aligned}$$

Similarly, when  $(2k+1)T \leq t \leq (2k+2)T$

$$\begin{aligned} z_2(t) &= \sqrt{\frac{2}{E_s\hat{T}}} \int_{(2k+1)\hat{T}}^{(2k+2)\hat{T}} \mathbf{y}(t) \cos\left(\frac{\pi t}{\hat{T}}\right) dt \\ &\quad + \sqrt{\frac{2}{E_s\hat{T}}} \int_{(2k+2)T}^{(2k+2)T+\hat{T}} \mathbf{y}(t) \cos\left(\frac{\pi t}{\hat{T}}\right) dt \end{aligned}$$

from which it follows through similar techniques when deriving  $z_1(t)$  that

$$\begin{aligned} z_2(t) &= \frac{1}{\sqrt{T\hat{T}}} \begin{bmatrix} -h_{11}(k) + h_{11}(k+1)\alpha_{a_{4k}} + h_{12}(k) + h_{12}(k+1)\alpha_{a_{4k+1}} \\ -h_{21}(k) + h_{21}(k+1)\alpha_{a_{4k}} + h_{22}(k) + h_{22}(k+1)\alpha_{a_{4k+1}} \end{bmatrix} \\ &\quad + \sqrt{\frac{2}{E_s\hat{T}}} \begin{bmatrix} \int_{(2k+1)\hat{T}}^{(2k+2)\hat{T}} n_1(t) \cos\left(\frac{\pi t}{\hat{T}}\right) dt \\ \int_{(2k+1)\hat{T}}^{(2k+2)\hat{T}} n_2(t) \cos\left(\frac{\pi t}{\hat{T}}\right) dt \end{bmatrix} \end{aligned}$$

### III) Timing Offset Synchronization Error

In addition to loses orthogonality, the presence of timing offset can cause channel coefficients of adjacent symbol periods to leak in to the current estimate. This is now shown by considering the following two cases.

i)  $T_o(t) > 0$ . Then for  $2kT \leq t \leq (2k+1)T$

$$\mathbf{z}_1(t) = \sqrt{\frac{2}{E_s T}} \left( \int_{2kT+|T_o|}^{(2k+1)T} \mathbf{y}(t) \cos\left(\frac{\pi t}{T}\right) dt + \int_{(2k+1)T}^{(2k+1)T+|T_o|} \mathbf{y}(t) \cos\left(\frac{\pi t}{T}\right) dt \right)$$

from which it follows after several manipulations that

$$\begin{aligned} \mathbf{z}_1(t) &= \frac{1}{T} \begin{bmatrix} h_{11}(k) (\beta_{a_{2k}} - \gamma_{a_{2k}}) + h_{12}(k) (\beta_{a_{2k+1}} + \gamma_{a_{2k+1}}) \\ h_{21}(k) (\beta_{a_{2k}} - \gamma_{a_{2k}}) + h_{22}(k) (\beta_{a_{2k+1}} + \gamma_{a_{2k+1}}) \end{bmatrix} \\ &+ \sqrt{\frac{2}{E_s T}} \begin{bmatrix} \int_{2kT+|T_o|}^{(2k+1)T+|T_o|} n_1(t) \cos\left(\frac{\pi t}{T}\right) dt \\ \int_{2kT+|T_o|}^{(2k+1)T+|T_o|} n_2(t) \cos\left(\frac{\pi t}{T}\right) dt \end{bmatrix} \end{aligned}$$

where

$$\beta_i = T - |T_o| \left( 1 + \exp\left(j \frac{(-1)^i \pi |T_o|}{T}\right) \right) \text{sinc}\left(\frac{|T_o|}{T}\right)$$

and

$$\gamma_i = |T_o| \left( 1 + \exp\left(j \frac{(-1)^i \pi |T_o|}{T}\right) \right) \text{sinc}\left(\frac{|T_o|}{T}\right).$$

For  $(2k+1)T \leq t \leq (2k+2)T$

$$\begin{aligned} \mathbf{z}_2(t) &= \sqrt{\frac{2}{E_s T}} \int_{(2k+1)T+|T_o|}^{(2k+2)T} \mathbf{y}(t) \cos\left(\frac{\pi t}{T}\right) dt + \\ &\sqrt{\frac{2}{E_s T}} \int_{(2k+2)T}^{(2k+2)T+|T_o|} \mathbf{y}(t) \cos\left(\frac{\pi t}{T}\right) dt \end{aligned}$$

from which it follows from similar techniques when deriving  $\mathbf{z}_1(t)$  that

$$\begin{aligned} \mathbf{z}_2(t) &= \frac{1}{T} \begin{bmatrix} -h_{11}(k) \beta_{a_{2k}} + h_{11}(k+1) \gamma_{a_{2k}} + h_{12}(k) \beta_{a_{2k+1}} + h_{12}(k+1) \gamma_{a_{2k+1}} \\ -h_{21}(k) \beta_{a_{2k}} + h_{21}(k+1) \gamma_{a_{2k}} + h_{22}(k) \beta_{a_{2k+1}} + h_{22}(k+1) \gamma_{a_{2k+1}} \end{bmatrix} \\ &+ \sqrt{\frac{2}{E_s T}} \begin{bmatrix} \int_{(2k+1)T+|T_o|}^{(2k+2)T+|T_o|} n_1(t) \cos\left(\frac{\pi t}{T}\right) dt \\ \int_{(2k+1)T+|T_o|}^{(2k+2)T+|T_o|} n_2(t) \cos\left(\frac{\pi t}{T}\right) dt \end{bmatrix} \end{aligned}$$

ii)  $T_o(t) < 0$ . When  $2kT \leq t \leq (2k+1)T$

$$\mathbf{z}_1(t) = \sqrt{\frac{2}{E_s T}} \left( \int_{2kT-|T_o|}^{2kT} \mathbf{y}(t) \cos\left(\frac{\pi t}{T}\right) dt + \int_{2kT}^{(2k+1)T-|T_o|} \mathbf{y}(t) \cos\left(\frac{\pi t}{T}\right) dt \right)$$

from which one can show after some effort that

$$\begin{aligned} \mathbf{z}_1(t) &= \frac{1}{T} \begin{bmatrix} -h_{11}(k-1) \delta_{a_{2k}} + h_{11}(k) \zeta_{a_{2k}} + h_{12}(k-1) \delta_{a_{2k+1}} + h_{12}(k) \zeta_{a_{2k+1}} \\ -h_{21}(k-1) \delta_{a_{2k}} + h_{21}(k) \zeta_{a_{2k}} + h_{22}(k-1) \delta_{a_{2k+1}} + h_{22}(k) \zeta_{a_{2k+1}} \end{bmatrix} \\ &+ \sqrt{\frac{2}{E_s T}} \begin{bmatrix} \int_{2kT-|T_o|}^{(2k+1)T-|T_o|} n_1(t) \cos\left(\frac{\pi t}{T}\right) dt \\ \int_{2kT-|T_o|}^{(2k+1)T-|T_o|} n_2(t) \cos\left(\frac{\pi t}{T}\right) dt \end{bmatrix} \end{aligned}$$

where

$$\delta_i = |T_o| + (T - |T_o|) \left( 1 + \exp \left( j \frac{(-1)^i \pi (T - |T_o|)}{T} \right) \right) \operatorname{sinc} \left( \frac{T - |T_o|}{T} \right)$$

and

$$\zeta_i = T - |T_o| + (T - |T_o|) \left( 1 + \exp \left( j \frac{(-1)^i \pi (T - |T_o|)}{T} \right) \right) \operatorname{sinc} \left( \frac{T - |T_o|}{T} \right).$$

For  $(2k+1)T \leq t \leq (2k+2)T$

$$\begin{aligned} z_2(t) &= \sqrt{\frac{2}{E_s T}} \int_{(2k+1)T-|T_o|}^{(2k+1)T} \mathbf{y}(t) \cos \left( \frac{\pi t}{T} \right) dt \\ &+ \sqrt{\frac{2}{E_s T}} \int_{(2k+1)T}^{(2k+2)T-|T_o|} \mathbf{y}(t) \cos \left( \frac{\pi t}{T} \right) dt \end{aligned}$$

and one can arrive using similar techniques as the formulation of  $z_1(t)$  at

$$\begin{aligned} z_2(t) &= \frac{1}{T} \begin{bmatrix} h_{11}(k) (\delta_{a_{2k}} - \zeta_{a_{2k}}) + h_{12}(k) (\delta_{a_{2k+1}} + \zeta_{a_{2k+1}}) \\ h_{21}(k) (\delta_{a_{2k}} - \zeta_{a_{2k}}) + h_{22}(k) (\delta_{a_{2k+1}} + \zeta_{a_{2k+1}}) \end{bmatrix} \\ &+ \sqrt{\frac{2}{E_s T}} \begin{bmatrix} \int_{(2k+1)T-|T_o|}^{(2k+2)T-|T_o|} n_1(t) \cos \left( \frac{\pi t}{T} \right) dt \\ \int_{(2k+1)T-|T_o|}^{(2k+2)T-|T_o|} n_2(t) \cos \left( \frac{\pi t}{T} \right) dt \end{bmatrix}. \end{aligned}$$

After analyzing  $z_1(t)$  and  $z_2(t)$  for all cases of synchronization error, it is clear that significant timing offsets and/or errors in the symbol period degrade the quality of channel estimation. Depending on the sign of  $T_o$  and  $\epsilon$ , leakage of previous or future channel coefficients into the current CSI estimate play a significant role.

## - Detection

Now that the receiver has an estimate of the channel matrix, the second stage of the STBC receiver is the detection process. In order to draw from the orthogonal design of the proposed STBC some preparation is needed. Denoting  $2kT \leq \lambda \leq (2k+1)T$  and  $0 \leq \tau \leq T$ , the received waveform vector is concatenated to form

$$\begin{aligned} \mathbf{y}(\tau) &\triangleq \begin{bmatrix} \mathbf{y}(\lambda) \\ \mathbf{y}^*(\lambda + T) \end{bmatrix} = \begin{bmatrix} \hat{h}_{11}(k) & \hat{h}_{12}(k) \\ \hat{h}_{21}(k) & \hat{h}_{22}(k) \\ \hat{h}_{12}^*(k) & -\hat{h}_{11}^*(k) \\ \hat{h}_{22}^*(k) & -\hat{h}_{21}^*(k) \end{bmatrix} \begin{bmatrix} x_1(\tau) \\ x_2(\tau) \end{bmatrix} + \begin{bmatrix} n_1(\lambda) \\ n_2(\lambda) \\ n_1^*(\lambda + T) \\ n_2^*(\lambda + T) \end{bmatrix} \\ &= \widehat{\mathbf{H}}_{eff}(k) \mathbf{x}(\tau) + \boldsymbol{\eta}(\tau) \end{aligned}$$

Then

$$\bar{\mathbf{y}}(k) \triangleq j \int_0^T \mathbf{y}(\tau) \sin \left( \frac{\pi \tau}{T} \right) d\tau = \widehat{\mathbf{H}}_{eff}(k) \bar{\mathbf{x}}(k) + \bar{\boldsymbol{\eta}}(k) \quad (2)$$

where

$$\bar{\mathbf{x}}_n(k) = \begin{cases} 1 & \text{if } s_1(t) \text{ was sent} \\ -1 & \text{otherwise} \end{cases}$$

Noting that  $\widehat{\mathbf{H}}(k)_{eff}^H \widehat{\mathbf{H}}(k)_{eff} = \|\widehat{\mathbf{H}}(k)\|_F^2 \mathbf{I}_{N_t}$ , the decoupled received symbol vector is

$$\widehat{\mathbf{x}}(k) = \widehat{\mathbf{H}}_{eff}(k)^H \overline{\mathbf{y}}(k) = \|\widehat{\mathbf{H}}(k)\|_F^2 \overline{\mathbf{x}}(k) + \widetilde{\mathbf{n}}(k),$$

where  $\widetilde{\mathbf{n}}(k) = \widehat{\mathbf{H}}_{eff}(k)^H \mathbf{n}(k)$ . The minimum distance decision is

$$\widehat{x}_i(k) = \arg \min_{x_i \in \{-1, 1\}} \|\widehat{x}_i(k) - \|\widehat{\mathbf{H}}(k)\|_F^2 x_i(k)\|^2 \quad i = 1, 2.$$

In addition to errors in the channel estimation stage, the presence of synchronization errors will negatively impact the calculation of (2). The procedure is identical to the one taken in the channel estimation stage and will not be pursued. The effects also will be similar in that  $\overline{x}_n(k)$  will deviate from the values of  $\pm 1$ .

## SIMULATION RESULTS

To estimate the impact of synchronization errors on the system symbol error rate, a number of simulations were run. The results of these simulations are summarized in Figures 1-3. In all cases the transmitter had two transmit antennas, and sent FSK modulated data. The channel imposed fading following a Jake's model, and added white Gaussian noise. The receiver also used two antennas. After estimating the channel coefficients, the receiver demodulated the data with a variety of errors imposed on it.

In Fig 1 the receiver used the correct symbol error rate, but had a constant time offset which forced a controlled amount of ISI. The various curves show the effect of static errors from zero to 10 percent of the symbol time, where the synchronization error imposed a penalty of approximately 2.5 dB. The curves were fit to simulations run every one dB. All simulations generated at least 100 errors.

The curves in Fig 1 may be appropriate to use when there is a bias in the symbol synchronization device, or the symbol sync loop is somehow stressed. Perhaps a more common problem is when channel noise causes the symbol synchronization device to make random errors. The results of such a simulation are shown in Fig 2. The phase error was modeled as a first order, autoregressive, Gaussian process. The statistics listed on the right side of the plot indicate the standard deviation of this error process, as a percentage of a symbol time. When the standard deviation of the synchronization error is 10 percent of a symbol time, the BER curve degrades by approximately 3 dB.

The final simulation executed modeled the effects of a mis-match in the symbol rate between the transmitter and receiver. Symbol rate errors up to 20 percent were simulated, and the results displayed in Fig 3.

## CONCLUSION

The impact of symbol synchronization errors in MIMO communication systems was analyzed both mathematically, and through computer simulation. Small synchronization errors do not cause a catastrophic failure of the MIMO receivers, but can have a significant impact on the overall system performance. The simulations were written in MATLAB<sup>TM</sup>, using commonly available toolboxes. The source code can be obtained by contacting any of the authors.



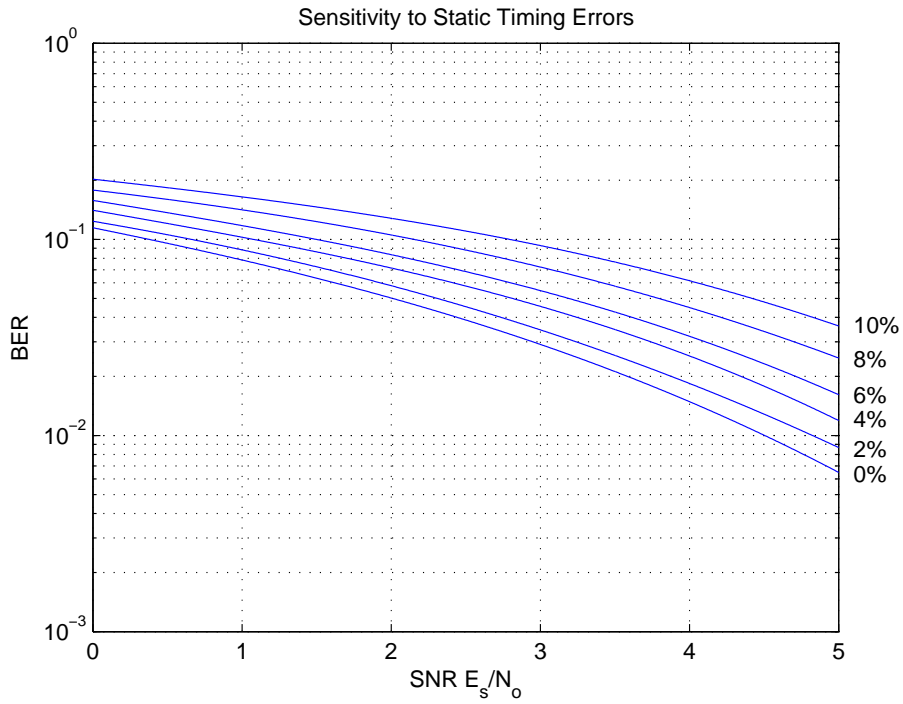


Figure 1: Static Timing Errors

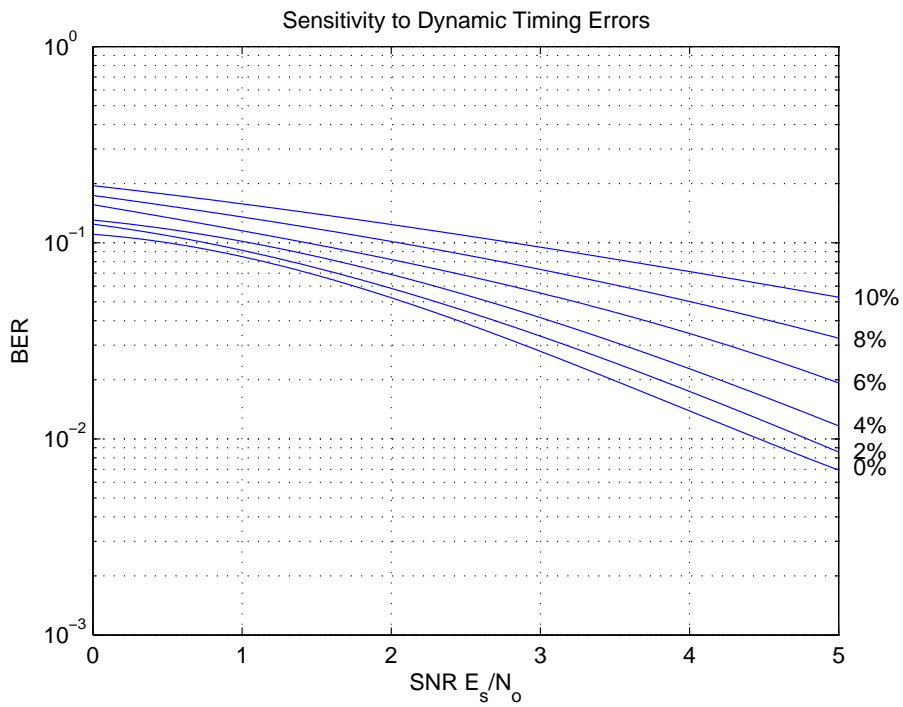


Figure 2: Gaussian Distributed Timing Errors

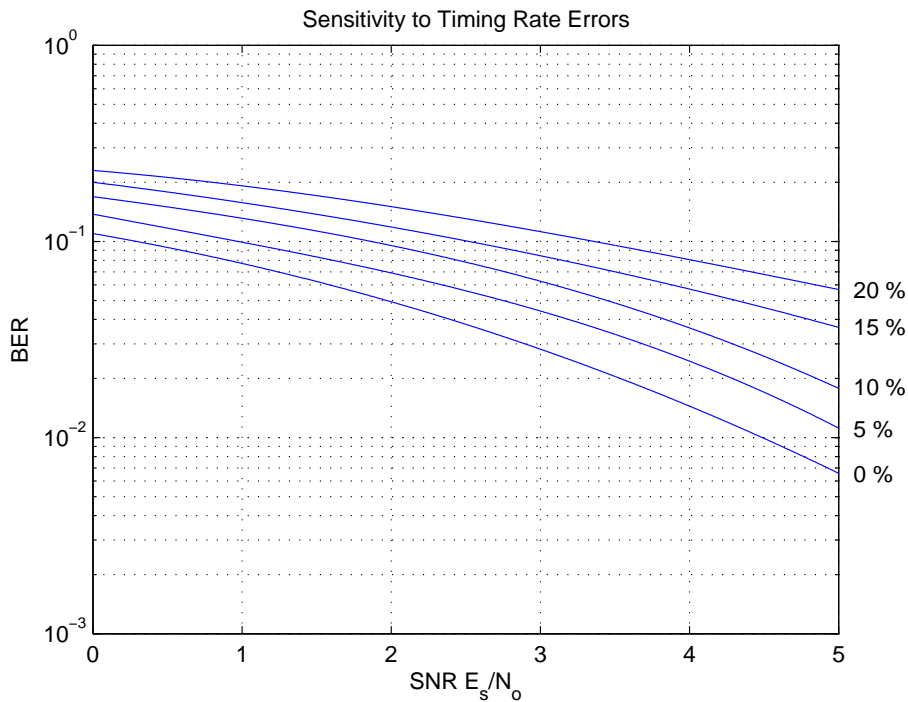


Figure 3: Static Symbol Rate Errors

## REFERENCES

- [1] E. Telatar, "Capacity of multi-antenna gaussian channels," *AT&T Bell Laboratories Internal Tech. Memo.*, Jun. 1995.
- [2] G. Foschini, "Layered space-time architecture for wireless communication in a fading environment when using multi-element antennas," *Bell Labs Syst. Tech. J.*, vol. 1, no. 2, pp. 41–59, 1996.
- [3] A. Goldsmith, *Wireless Communications*. New York: Cambridge University Press, 2005.
- [4] D. Tse and P. Viswanath, *Fundamental of Wireless Communication*. New York, NY: Cambridge University Press, 2005.
- [5] C. Potter and K. Kosbar, "Modeling channel estimation error in continuously varying mimo channels," *Proceedings of the International Telemetering Conference*, Oct. 2007.
- [6] P. Ho, X. Zhang, and P. Y. Kam, "A space-time block code using orthogonal frequency shift keying," *Proc. IEEE International Conference on Communications (ICC'05)*, vol. 5, pp. 2896–2900, May 2005.
- [7] A. Jazwinski, *Stochastic Process and Filtering Theory*. Academic Press, 1993.
- [8] J. G. Proakis, *Digital Communications*. New York, NY: Mc-Graw-Hill, Inc., 1995.
- [9] S. Alamouti, "A simple transmit diversity technique for wireless communications," *IEEE J. Sel. Areas Commun.*, vol. 16, pp. 1451–1458, Aug. 1998.